ORIGINAL ARTICLE

A 2D metal-organic coordination polymer of Cu(II) based on tartrate ligands; synthesis, characterization, spectroscopic, crystal structure, solution studies and electrochemical behavior

Marzieh Rashidipour [a], Zohreh Derikvand [b,*], Ardeshir Shokrollahi [c], Zahra Mohammadpour [c], Azadeh Azadbakht [b]

[a] *Khorram Abad Branch, Young Researchers Club, Islamic Azad University, Lorestan, Iran*
[b] *Department of Chemistry, Faculty of Science, Khorramabad Branch, Islamic Azad University, Khorramabad, Iran*
[c] *Department of Chemistry, Yasouj University, Yasouj, Iran*

Abstract A chiral 2D coordination polymer, $\{[Cu_2(tart)_2(H_2O)_2]\cdot 4H_2O\}_n$ **1**, was synthesized by the reaction of tartaric acid (tartH$_2$), acridine (acr) and Cu(NO$_3$)$_2$ and characterized by elemental analysis, spectral (IR, UV–Vis), electrochemical and X-ray single crystal diffraction. The acridine has not been incorporated in the crystal structure. Compound **1** has infinite two-dimensional network and such 2D networks were linked by complicated O−H···O hydrogen bonds to form 3D supramolecular network. In this polymer the tartrate ligands chelate two Cu(II) atoms at opposite ends using one carboxylate oxygen atom and one hydroxyl oxygen atom therefore each Cu(II) atom is chelated by two halves of tartrate dianions. The Cu1 and Cu2 centers are coordinated by five oxygen atoms from two tartrate ligands and one oxygen atom of water molecule therefore both Cu(II) centers adopt distorted octahedral geometries. The protonation constants of tartaric acid (tart) and acridine (acr), in all of the probability protonated forms, the equilibrium constants for the tart–acr proton transfer system and the stoichiometry and stability constant of the complexation of this system with Cu^{2+} ion in dioxane/water (1:1 V/V) solvent were investigated by the potentiometric pH titration method. The stoichiometries of the complex species in solution were compared with the corresponding crystalline complex.

© 2013 King Saud University. Production and hosting by Elsevier B.V. All rights reserved.

* Corresponding author. Tel./fax: +98 661 6200399.
E-mail address: zderik@yahoo.com (Z. Derikvand).

1. Introduction

The design of metal organic coordination polymers (MOCPs) has attracted great interests not only for their potential applications in catalysis, storage, conduction, non-linear optics (NLOs), luminescence, ferroelectricity and magnetism, but

also for their captivating architectures and topologies (Eddaoudi et al., 2001; Batten and Robson, 1998; Férey, 2008; Moulton and Zaworotko, 2001; Vittal, 2007; James, 2003; Zhang and Chen, 2008; Kitagawa et al., 2004; Zhang et al., 2009). Construction of chiral coordination polymers from organic molecules and metal ions have attracted considerable attention due to their intriguing structures and potential utility in asymmetric catalysis (Seo et al., 2000; Fujita et al., 1994; Sawaki et al., 1998) chiral separation (Evans et al., 2001; Kepert et al., 2000) and nonlinear optical materials (Xiong et al., 2001; Holman et al., 2001; Wu et al., 2003). For this intention choosing a good ligand is very important. Tartaric acid (hereafter tartH$_2$) is a colorless, diprotic organic acid that occurs naturally in many plants, particularly grapes, bananas, and tamarinds, and is one of the main acids found in wine. It has many applications such as in making silver mirrors, in the manufacture of soft drinks, to provide tartness to foods, in tanning leather, and in making blueprints also tartaric acid has optical activity (Synoradzki et al., 2008). The tartH$_2$ as carboxylate derivative has drawn extensive attention in coordination chemistry (Al-Dajani et al., 2010; Meng et al., 2008). This ligand has been used as building blocks to construct 1D, 2D and 3D frameworks due to the diversity of binding modes of the carboxyl group and hydroxyl group in the tartaric acid (Meng et al., 2008; Du and Han, 2011; McCanq et al., 1997).

Herein, we described the synthesis, characterization, spectroscopic, crystal structures, electrochemical behavior of a chiral 2D metal–organic coordination polymer, $\{[Cu_2(tart)_2 (H_2O)_2]\cdot4H_2O\}_n$ **1**. In addition the behavior of Cu^{2+} in the presence of tartH$_2$/acr 1:1 M mixtures in dioxin/water (1:1 V/V) solution has also been investigated.

2. Experimental

2.1. General methods and materials

All materials were purchased from Merck. Solvents used throughout the reactions were of high purity. IR spectroscopy was performed applying on a Perkin-Elmer Spectrum RXI FT-IR spectrophotometer in the 4000–400 cm^{-1} region using KBr pellet.

Elemental analysis was performed with a Heraus CHN Pro apparatus. The X-ray data was obtained with a Bruker SMART 1000 CCD diffractometer. The UV–Vis spectrum of the polymer was recorded on a JELWAY 6505 UV–Vis spectrophotometer in the range of 200–900 nm at room temperature. A Model 794 Metrohm Basic Titrino was attached to an extension combined glass–calomel electrode mounted in an air-protected, sealed, thermostated jacketed cell maintained at 25.0 ± 0.1 °C by circulating water, from a constant-temperature bath Fisherbrand model FBH604, LAUDA, Germany, equipped with a stirrer and a 10.000-ml-capacity Metrohm piston buret. The pH meter-electrode system was calibrated to read −log[H$^+$]. Electrochemical experiments were performed using an Autolab modular electrochemical system (Eco Chem., Utrecht, The Netherlands) equipped with PSTA 20 model and driven by GPES software (Eco Chem.). A conventional three-electrode cell was used with a saturated Ag|AgCl as reference electrode, a Pt wire as counter electrode and a modified carbon paste as working electrode. All experiments were carried out at ambient temperature of 20 ± 1 °C. A Metrohm pH-meter (model 691) was also applied for the pH measurements.

2.2. Synthesis of $\{[Cu_2(tart)_2(H_2O)_2]\cdot4H_2O\}_n(\mathbf{1})$

An aqueous solution of Cu(NO$_3$)$_2$.3H$_2$O (120 mg, 0.5 mmol) in water (5 mL) was added to a solution of tartaric acid (150 mg, 1 mmol) in water (20 mL) and acridine (358 mg, 2 mmol) in methanol (5 mL) under stirring in a 1:2:4 M ratio, shown in Scheme 1. The solution was heated very slightly (80 °C) for 1 h. After 2 weeks, prism blue crystals of the polymer were obtained by slow evaporation of the solvent at room temperature. *Anal*. Calc. for C$_8$H$_{20}$Cu$_2$O$_{18}$: C, 18.06; H, 3.76. Found; C, 18.04; H, 3.78%. **IR** (KBr disk, v/cm^{-1}): 3415 (s), 3357(s), 3103(b), 2976(s), 2786 (w), 2643(w), 2568(w), 1621(s, sh), 1580(s), 1433(s), 1390(s), 1365 (s), 1327(s), 1301(m), 1274(s), 1220(s), 1101(w), 1074(s),1060(s), 1012(s), 943(w), 917(m), 888(m), 824(s), 795(m), 748(s), 688(m), 645(s), 539(s), 489(s), 428(s). UV–Vis (aqueous solution) (λ, nm): 730.

2.3. Crystal structure determination and refinement

Unit cell determination and data collection of the polymer were collected on a Bruker SMART 1000 CCD area detector system (Bruker, 2007) using the Mo Kα radiation (λ = 0.71073 Å). The structure was solved and refined by full-matrix least-squares techniques on F^2 using SHELX-98 (SHELXL program package) (Sheldrick, 2008). The absorption correction type was multi-scan. The hydrogen atoms bonded to O atoms (further H(O)) were found in difference Fourier synthesis. The H(C) atom positions were calculated. The H(O) hydrogen atoms were refined in
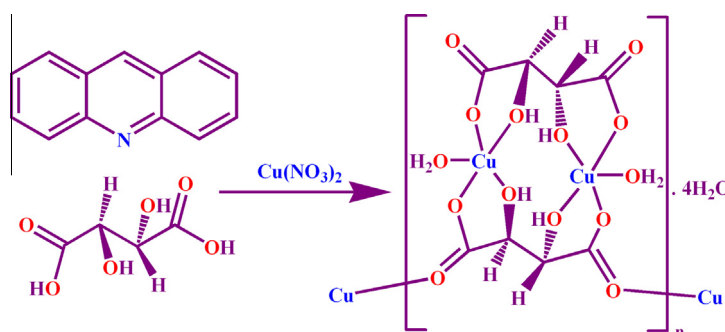
Scheme 1   Preparation route of compound **1**.

isotropic approximation with O−H distances restrained to 0.85 Å, the H(C) atoms were refined in the riding model. The isotropic thermal parameters of hydrogen atoms were set to 1.2 U_{eq}(A), where U(A) is the equivalent thermal parameters of the atom to which corresponding H atom is bonded.

2.4. Potentiometric measurements

The jacketed cell containing test solution was equipped with a magnetic stirrer and a tightly fitting cap, through which the electrode system and 10-ml capacity Metrohm piston buret were inserted and sealed with clamps and O-rings. The atmospheric CO_2 was excluded from the titration cell with a purging steam of purified nitrogen gas. The concentration of tart and acr was set at 3.33×10^{-3} M, for the potentiometric pH titrations of tart, acr and tart–acr in the absence and presence of 1.67×10^{-3} M metal ion. A standard carbonate-free NaOH solution (0.0968 M) was used in all titrations. The ionic strength was adjusted to 0.1 M with $NaClO_4$. Before an experimental point (pH) was measured, sufficient time was undergone for the establishment of the equilibrium. Protonation constants of ligands and stability constants of proton transfer system and their metal complexes were evaluated using the *BEST* program described by Martell and Motekaitis (1992). The value of autoprotolysis constant for dioxane/water (1:1 V/V) solvent (Ks = [H$^+$][OH$^-$]) was calculated according to the literature (Martell and Motekaitis, 1992).

3. Results and discussion

3.1. The spectroscopic studies

The IR spectrum of compound **1** shows an intense band at 3415 cm^{-1} attributed to the hydroxyl groups of tartrate ligands, which are involved both in the intra and intermolecular hydrogen bonds. The spectrum exhibits also the bands at 3357, 3103, and 2976 cm^{-1} indicating several hydrogen bonding interactions between water molecules and carboxyl groups in **1**. The IR spectrum of the polymer exhibits no absorption near 1700 cm^{-1}, confirming the complete deprotonation of the carboxyl groups. The carboxylic groups exhibit strong bands in the region 1621–1580 cm^{-1}. The bands in 1621 and 1390 cm^{-1} correspond to the asymmetric and symmetric stretching of carboxyl groups, respectively. The value of $\Delta[\nu_{as} - \nu_s]$ is 231 cm^{-1}, comparatively larger than 200 cm^{-1}, indicating the monochelation of the carboxylic group to the metal ion (Shi et al., 2006). The bands at 489 and 428 cm^{-1} are attributed to the Cu–O vibrations.

3.2. Description of the crystal structure

The crystal structure of the title compound was previously reported by other authors (Jian et al., 2005) but here we provided some details of solid state packing. The single crystal X-ray diffraction analysis shows that **1** crystallized in the monoclinic space group $P2_1$ with a chiral 2D network. The crystallographic data, bond lengths and angles and selected intermolecular hydrogen bond parameters are listed in Tables 1–3, respectively. The molecular structure with atom numbering of **1** is presented in Fig. 1. As shown in Fig. 1 each tartrate chelates two Cu(II) atoms at opposite ends using one carboxylate oxygen atom and one hydroxyl oxygen atom. Therefore each

Table 1 Crystallographic data for **1**.

Compound	**1**
Empirical formula	$C_8H_{20}Cu_2O_{18}$
Formula weight	531.32
Crystal system	Monoclinic
Space group	$P2_1$
a (Å)	8.3488(10)
b (Å)	8.7335(11)
c (Å)	12.0342(15)
α (°)	90
β (°)	104.104(2)
γ (°)	90
Z	2
V (Å^3)	851.01(18)
D_{calc} (Mg m^{-3})	2.073
$F(0\,0\,0)$	540
Reflections	9877
R_{int}	0.0317
Theta range (°)	1.74–30.03
Goodness-of-fit on F^2	1.003
Final R indices [$I > 2\sigma(I)$]	$R_1 = 0.0325$, $wR_2 = 0.0758$
R indices (all data)	$R_1 = 0.0398$, $wR_2 = 0.0801$

Table 2 Selected bond lengths (Å) and angles (°) for **1**.

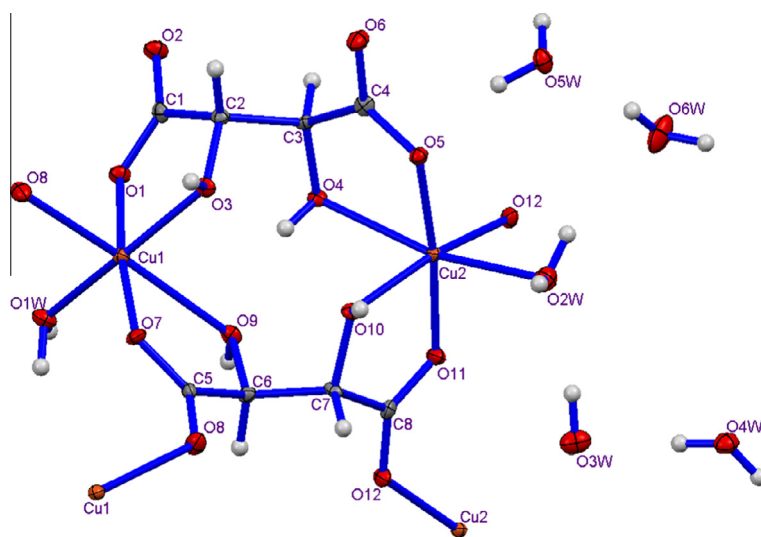| Bond distances			
Cu1–O7	1.921 (2)	Cu2–O5	1.935 (2)
Cu1–O1	1.934 (2)	Cu2–O11	1.937 (2)
Cu1–O1W	1.974 (2)	Cu2–O12^{ii}	1.972 (2)
Cu1–O3	2.007 (2)	Cu2–O10	2.025 (2)
Cu1–O8^i	2.317 (2)	Cu2–O2W	2.356 (2)
Cu1–O9	2.425 (2)	Cu2–O4	2.409 (2)
Bond angles			
O7–Cu1–O1	173.13 (9)	O5–Cu2–O11	172.94 (9)
O7–Cu1–O1W	95.07 (10)	O5–Cu2–O12^{ii}	99.62 (9)
O1–Cu1–O1W	89.73 (9)	O11–Cu2–O12^{ii}	86.91 (9)
O7–Cu1–O3	92.24 (9)	O5–Cu2–O10	92.27 (8)
O1–Cu1–O3	82.55 (9)	O11–Cu2–O10	81.03 (9)
O1W–Cu1–O3	170.96 (9)	O12^{ii}–Cu2–O10	167.45 (9)
O7–Cu1–O8^i	94.65 (8)	O5–Cu2–O2W	88.42 (9)
O1–Cu1–O8^i	90.08 (9)	O12^{ii}–Cu2–O2W	85.95 (8)
O1W–Cu1–O8^i	91.97 (9)	O10–Cu2–O2W	98.44 (9)
O3–Cu1–O8^i	92.74 (8)	O5–Cu2–O4	76.97 (8)
O7–Cu1–O9	75.82 (8)	O11–Cu2–O4	99.81 (8)
O1–Cu1–O9	99.16 (8)	O12^{ii}–Cu2–O4	96.23 (8)
O1W–Cu1–O9	91.85 (9)	O10–Cu2–O4	82.50 (8)
O3–Cu1–O9	84.78 (8)	O2W–Cu2–O4	165.39 (8)
O8i–Cu1–O9	170.01 (8)		

Symmetry codes: (i) $-x$, $y + 1/2$, $-z$; (ii) $-x + 1$, $y + 1/2$, $-z + 1$.

Cu(II) atom is chelated by two halves of tartrate dianions. One of the tartrate ligands bridges two Cu(II) atoms and another one bridges four Cu(II) atoms to each other, forming 2D coordination polymer (Fig. 2). In **1**, the asymmetric unit contains two crystallographically independent Cu(II) centers. The Cu1 and Cu2 centers are coordinated by five oxygen atoms from two tartrate ligands and one oxygen atom of water molecule, (O1, O3, O7, O8A, O9 and O1W for Cu1 and O4, O5, O10, O11, O12A and O2W for Cu2 atom). Both Cu(II) centers adopt distorted octahedral geometries. Each Cu(II) atom in the dinuclear motif is coordinated in the axial posi-

Table 3 The hydrogen bond geometry of **1**.

| D–H$\cdots A$	D–H	H$\cdots A$	$D\cdots A$	D–H$\cdots A$
O1W–H1WB$\cdots$O4W[i]	0.844 (10)	1.859 (12)	2.693 (3)	169 (4)
O1W–H1WA$\cdots$O2[ii]	0.838 (10)	1.957 (18)	2.754 (3)	159 (4)
O2W–H2WA$\cdots$O6W	0.847 (10)	2.486 (17)	3.289 (4)	159 (3)
O2W–H2WB$\cdots$O6[iii]	0.856 (10)	1.866 (16)	2.694 (3)	162 (4)
O3–H3O$\cdots$O4W[iv]	0.847 (10)	1.856 (14)	2.680 (3)	164 (3)
O3W–H3WB$\cdots$O4[v]	0.845 (10)	1.863 (11)	2.705 (3)	174 (4)
O3W–H3WA$\cdots$O2W	0.842 (10)	1.982 (17)	2.790 (4)	161 (4)
O4–H4O$\cdots$O9	0.837 (10)	2.02 (2)	2.738 (3)	144 (3)
O4–H4O$\cdots$O3	0.837 (10)	2.16 (3)	2.704 (3)	123 (3)
O4–H4O$\cdots$O10	0.837 (10)	2.52 (3)	2.938 (3)	112 (3)
O4W–H4WB$\cdots$O3W	0.850 (10)	1.904 (11)	2.754 (3)	178 (4)
O4W–H4WA$\cdots$O2[vi]	0.850 (10)	2.046 (15)	2.866 (3)	162 (3)
O5W–H5WB$\cdots$O5	0.850 (10)	1.936 (17)	2.746 (3)	159 (4)
O5W–H5WB$\cdots$O6	0.850 (10)	2.52 (3)	3.178 (3)	135 (3)
O5W–H5WA$\cdots$O3W[vii]	0.846 (10)	1.904 (16)	2.722 (3)	163 (4)
O6W–H6WA$\cdots$O1[viii]	0.844 (10)	1.965 (14)	2.795 (3)	168 (4)
O6W–H6WB$\cdots$O5W	0.850 (10)	1.915 (16)	2.735 (4)	162 (4)
O9–H9O$\cdots$O6W[v]	0.847 (10)	1.808 (11)	2.654 (3)	175 (4)
O10–H10O$\cdots$O5W[iii]	0.857 (10)	1.702 (11)	2.558 (3)	175 (4)

Symmetry codes: (i) $x, y, z - 1$; (ii) $-x + 1, y - 1/2, -z$; (iii) $-x, y - 1/2, -z + 1$; (iv) $-x, y + 1/2, -z + 1$; (v) $-x + 1, y - 1/2, -z + 1$; (vi) $x, y - 1, z + 1$; (vii) $x, y + 1, z$; (viii) $x, y, z + 1$.

Figure 1 View of repeating unit in the coordination polymer, **1**.

tions by O1, O7 and O5, O11, for Cu1 and Cu2, respectively, while the equatorial positions are taken by O3, O8A, O9, O1W for Cu1 and O4, O10, O12A, O2W for Cu2 atoms. The axial Cu–O distances are shorter than the equatorial Cu–O distances (Table 2). The Cu1–O1W bond distance [1.974(2) Å] is significantly shorter than the Cu2–O2W bond distance, [2.356(2) Å]. The bond angle around Cu(II) atoms involving *trans* pairs of donor atoms is in the range of 170.01(8)–173.13(9)° for Cu1 and 165.39(8)–172.94(9)° for Cu2, and in the range of 75.82(8)–99.16(8) for Cu1 and 76.98(8)–99.81(8)° for Cu2 for the *cis* pairs of donor atoms. The two Cu(II) atoms in **1** are alienated by a distance of 5.276 Å, representing no interaction between them and this distance. Water clusters (H$_2$O)$_n$ are studied to understand the anomalous behavior of bulk water

for probing its possible roles in the stabilization and function of biomolecules and designing new material (Joannopoulous, 2001; Atwood et al., 2001). As shown in Fig. 3 there are four uncoordinated and two coordinated water molecules in the asymmetric unit which connected *via* O–H···O hydrogen bond to each other and form six-membered chain water clusters. The O···O distances are in the range of 2.693(3)–3.289(4) Å, also in the structure of **1** the complicated network of strong O–H···O hydrogen bonds of crystal water molecules and polymeric complexes results in an interesting 2D sheet of structure as shown in Fig. 3. Hydrogen bonding between the water molecules [O1W, O2W, O3W, O4W, O5W and O6W] and oxygen atoms [O1, O2 and O5] of carboxylate groups of polymeric complex form two alternately annular R_5^4 (12) **I** and R_7^5 (17)
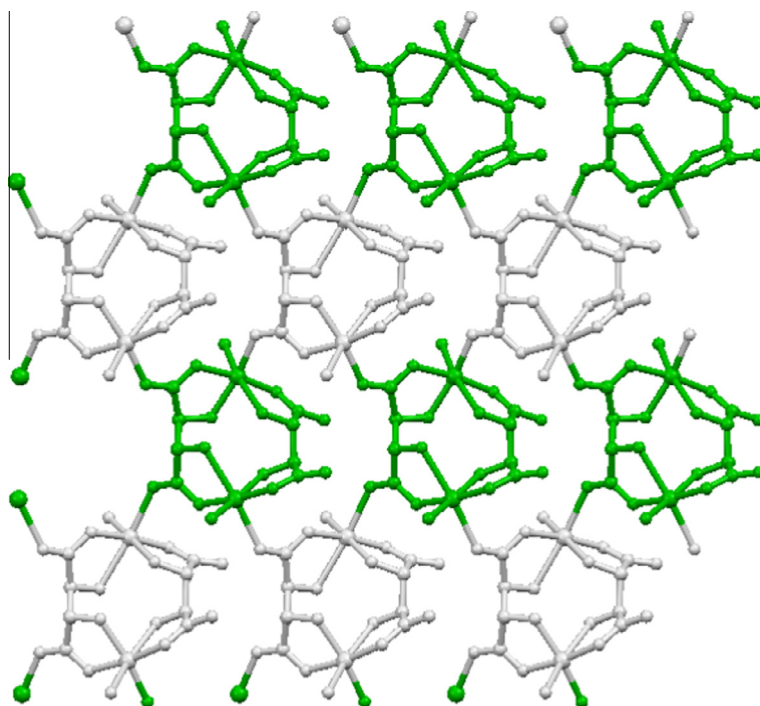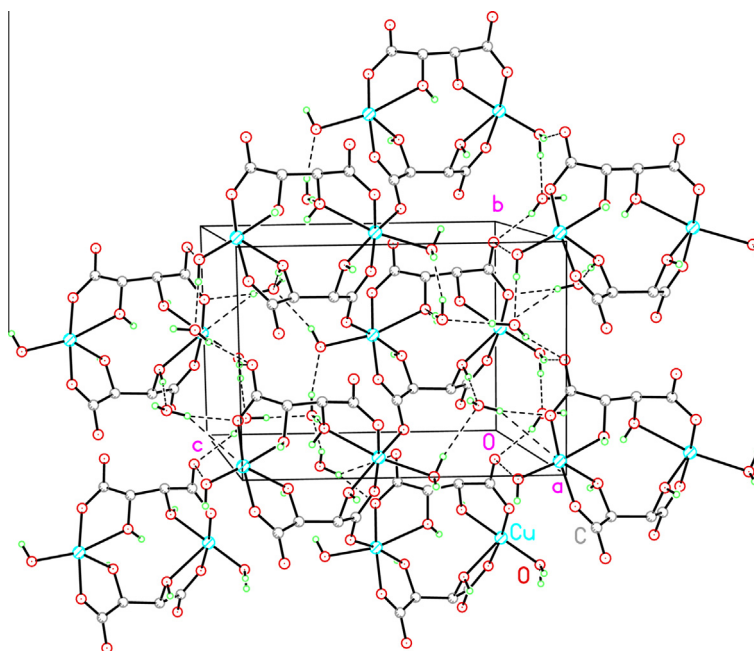
Figure 2   2D coordination network of **1** built up of tartrate and copper (II) ions.
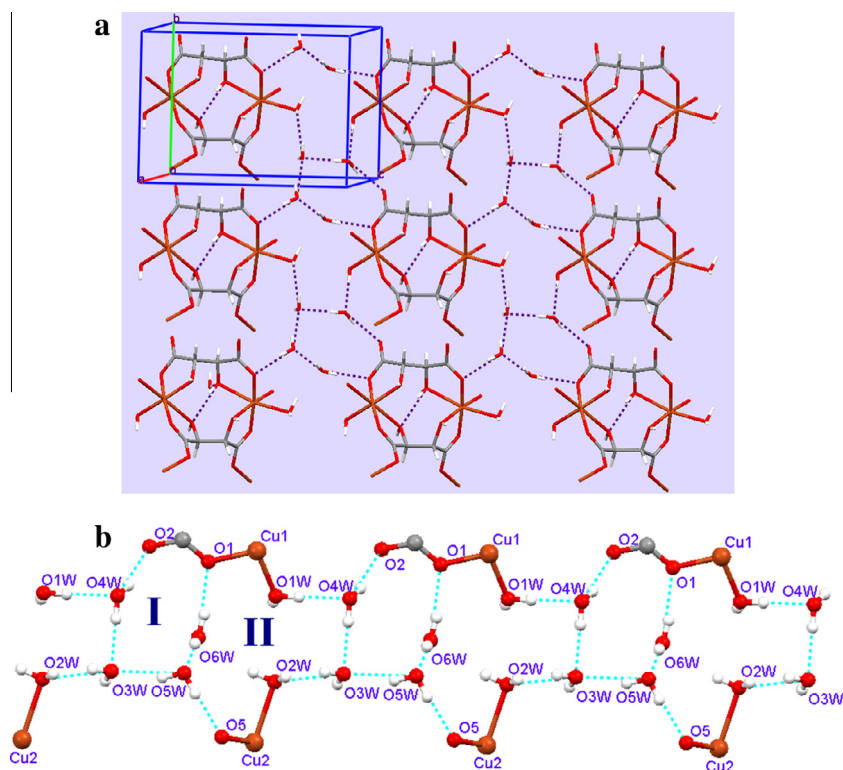
Figure 3   (a) A view of 2D sheets formed by O—H···O hydrogen bonds between polymeric complexes and crystal water molecules. Two fused R_5^4 (12) **I** and R_7^5 (17) **II** hydrogen-bonding motifs can be envisaged in the hydrogen-bonding pattern. (b) $(H_2O)_6$ water clusters formed by the lattice water molecules.

Figure 4   Packing diagram of **1**, showing the intermolecular hydrogen bonds in the 3D network.

II patterns. The hydrogen bond parameters are shown in Table 3. These hydrogen bond interactions extend the 2D chain structure of **1** to a 3D supramolecular network (Fig. 4).

3.3. Solution studies

It was discovered that acridine and some of its derivatives are slightly soluble in acidic and insoluble in neutral or alkaline aqueous solutions. These compounds are soluble in some organic solvents. Therefore, the solution study was achieved in dioxane/water (1:1 V/V) solvents as that has been reported in our previous works (Attar Gharamaleki et al., 2011; Mirzaei et al., 2011a,b).

The completely protonated forms of tart and acr as the building blocks of the proton transfer system, were titrated with a standard NaOH in a dioxane/water (1:1 V/V) solvent to obtain some information about their protonation constants preliminary. The result for tart is shown in Fig. 5a. The protonation constants of tart and acr in dioxane/water (1:1 V/V) solvent were calculated by fitting the potentiometric pH data to the BEST program. The

results are summarized in Table 4. The protonation constant of acr was reported in our previous paper (Mirzaei et al., 2011b). The observed difference between these results and those reported in aqueous solution for tart (Sajadi, 2010; Piispanen and Lajunen, 1995) and acr (Brown, 1955) is due to the condition of the solution and specially effect of solvent on the stability constants. Distribution diagram for tart is shown in Fig. 5b.

The determination of equilibrium constants for interactions between tart and acr in this medium was accomplished through the comparison of calculated and experimental pH profiles obtained with both tart and acr present in a 1:1 ratio, respectively, as described before (Sharif et al., 2006; Moghimi et al., 2005; English et al., 1997). The results are shown in Table 1. The corresponding species distribution diagram for tart–acr is shown in Fig. 6.

It is obvious that, the most abundant proton-transfer species present at pH > 6.9 (38.94%), 4.8 (25.94%), 4.2 (8.13%) and <2.5 (23.42%) are: [tart] [acr] ($\log K = 2.5$), {[tartH] [acr] ($\log K = 2.83$), [tart] [acrH] ($\log K = 3.23$)}, {[tartH] [acrH]
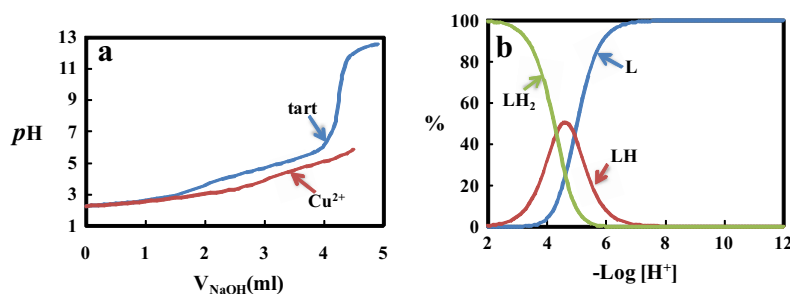
Figure 5   Potentiometric titration curves of tart (a) in the absence and presence of Cu^{2+} ion with NaOH 0.0968 M in dioxane/water (1:1 V/V) solution at 25 ± 0.1 °C and $\mu = 0.1$ M $NaClO_4$ and distribution diagram of tart (L) (b).

Table 4 Overall stability and stepwise protonation constants of tart, acr and recognition constants of tart with acr in several protonated forms in dioxane/water (1:1 V/V) solvent at 25 ± 0.1 °C and μ = 0.1 M NaClO$_4$.

Stoichiometry			$\log \beta$	Equilibrium quotient K	$\log K$	Max%	At pH
tart	acr	H					
1	0	1	4.94	–	4.94	50.39	4.6
1	0	2	9.26	–	4.32	99.52	< 2.4
0	1	1	4.54	–	4.56	99.7	< 2.5
1	1	0	2.5	–	2.5	38.94	> 6.9
				[tartacrH]/[tartH] [acr]	2.83		
1	1	1	7.77			25.94	4.8
				[tartacrH]/[tart] [acrH]	3.23		
1	1	2	11.74	[tartacrH$_2$]/[tartH] [acrH]	2.26	8.13	4.2
				[tartacrH$_2$]/[tartH$_2$] [acr]	2.48		
1	1	3	15.89	[tartacrH$_3$]/[tartH$_2$] [acrH]	2.09	23.42	< 2.5
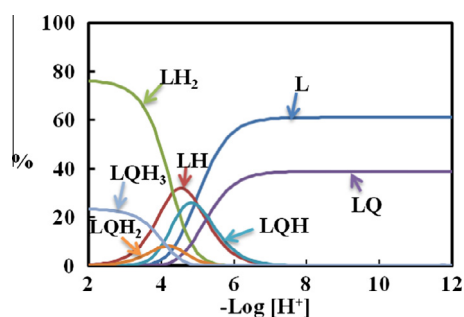
Figure 6 Distribution diagram of proton transfer interactions between tart (L) and acr (Q) in several protonated forms.

($\log K$ = 2.26), [tartH$_2$] [acr] ($\log K$ = 2.48)} and [tartH$_2$] [acrH] ($\log K$ = 2.09).

In order to evaluate the stoichiometry and stability constant of Cu^{2+} complexes with the tart–acr association in a dioxane/water (1:1 V/V) solvent, the equilibrium potentiometric pH titration profiles of tart, acr and their 1:1 mixture were obtained in the absence and presence of the Cu^{2+} ion. The resulting pH profiles are shown in Figs. 5a and 8a. It is seen from Figs. 5a and 8a that the titration of tart, acr and tart–acr in the presence of metal ions was stopped when the precipitate was observed.

The potentiometric titration curve of tart was depressed considerably in the presence of Cu^{2+} ion and the similar curve obtained from tart–acr–Cu^{2+} system, reveals that acr (Q) does not play an important role in the mix system. The extent of depression obviously depends on both the stoichiometries of resulting complexes and the ability of the metal ion to bind the binding sites of ligand. These results revealed that, Cu^{2+} ion has a weak interaction with acr, while forms much more stable complexes with tart and tart–acr systems.

The cumulative stability constants of $M_mL_lQ_qH_h$, β_{mlqh}, are defined in our previous publications (Sharif et al., 2006; Moghimi et al., 2005). There are M, L, Q and H as metal ion, tart, acr and proton, respectively and m, l, q, and h are the respective stoichiometric coefficients. The potentiometric pH titration curves of tart, acr (Mirzaei et al., 2011b) and their corresponding 1:1 mixture in the presence of Cu^{2+} ion were fitted to the BEST program in order to evaluate cumulative stability constants of the likely complex species in the solution.

The results are summarized in Table 5 and the corresponding distribution diagrams are shown in Figs. 7 and 8.

As it is obvious from Fig. 7 and Table 5 in the case of tart (L), as ligand, the most likely binary species for Cu^{2+} is: CuL, Cu$_2$L$_2$, CuLH$_{-1}$ and CuLH$_{-2}$. The species of Cu–acr was reported in the previous paper (Mirzaei et al., 2011a).

Fig. 8b and Table 5, revealed the formation of a variety of ternary complexes between the Cu^{2+} ion and the proton transfer system at different ranges of pH. The predominant species are MLQH (at pH 3.7) ternary species in the presence of M$_2$L$_2$ (at pH 4.5), ML (at pH 4.0–4.7), MLH$_{-2}$ (at pH > 8.1) and MLH$_{-1}$ (at pH 5.7) binary species. It is interesting to note that the isolated complex in the solid state is a binary complex (Cu$_2$L$_2$) which is observed in the solution with high abundance.

Table 5 Overall stability constants of tart/acr/Cu^{2+} ($q/l/m$) binary and ternary systems in a dioxane/water (1:1 V/V) solvent at 25 ± 0.1 °C and μ = 0.1 M NaClO$_4$.

System	m	l	q	h	$\log \beta$	Max%	At pH
Cu^{2+}–tart	1	1	0	0	5.10	29.42	4.0
	1	1	0	−1	0.34	68.02	5.8
	1	1	0	−2	−5.93	100	> 8.1
	1	2	0	0	7.33	Negligible	–
	1	2	0	1	8.50	Negligible	–
	2	2	0	0	13.52	61.1	4.0
Cu^{2+}–tart–acr	1	1	1	1	12.55	39.65	3.7
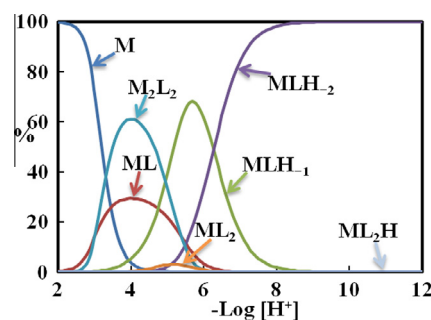
Figure 7 Distribution diagrams of tart(L)/M binary system. M = Cu^{2+}.
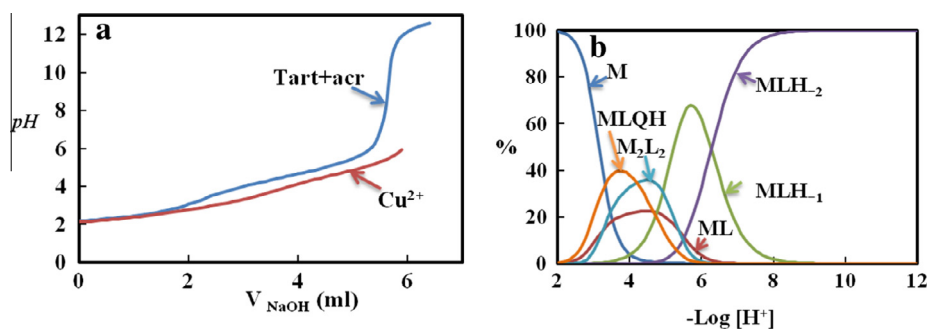
Figure 8 Potentiometric titration curves of tart + acr in the absence and presence of M^{n+} ion with NaOH 0.0968 M in dioxane/water (1:1 V/V) solution at 25 ± 0.1 °C and $\mu = 0.1$ M NaClO$_4$, M = Cu^{2+} (a) and distribution diagrams of tart(L)/acr(Q)/M ternary systems M = Cu^{2+} (b).
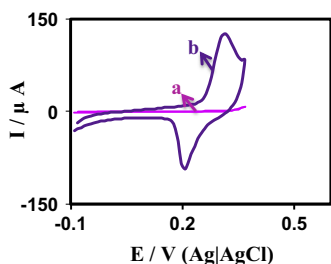
Figure 9 Cyclic voltammetric responses of unmodified carbon paste electrode (a) and **1–CPE** (b) at scan rate 50 mV s^{-1}.

3.4. UV–Vis spectra

Electronic spectra of the compound **1** were recorded in an aqueous solution from 200 to 900 nm. In the spectrum of **1**, a broad bond was observed at 730 nm which can be assigned to spin allowed d–d transition bonds ($^2E_g \rightarrow {}^2T_{2g}$) of copper (II) complex.

3.5. Electrochemical behaviors

Cyclic voltammograms of the Cu(II) polymer carbon paste electrode (**1−CPE**) were carried out at room temperature. The modified **1−CPE** was fabricated as follows: 10 mg of **1**, 50 mg graphite powder and proper amount of anhydrous ethanol were mixed to form a uniform mixture, which was left to evaporate the solvent at room temperature in the air. Then 20 ml paraffin oil was added to the graphite-**1** mixtures. The **1−CPE** was packed into a piston glass tube electrode (3 mm in diameter). Prior to the measurements the **1−CPE** was smoothed out on a piece of transparent paper to get a fresh surface. All the potentials reported in this work were versus Ag|AgCl electrode. Unmodified carbon paste electrode was prepared by adding 20 ml paraffin oil to 50 mg graphite powder. A cyclic voltammograms of modified **1−CPE** and unmodified carbon paste electrodes at scan rate of 50 mV s^{-1} are shown in Fig. 9. There is no redox peak at the surface of bare **CPE** in the potential range of −0.1 to 0.5 V. However, a reversible redox peak with formal potentials 0.26 V versus Ag|AgCl electrode is observed at **1−CPE**, which attributed to Cu^{II}/Cu^{I}.

4. Conclusion

We have synthesized and characterized a chiral 2D coordination polymer of Cu^{II} atom with tartrate ligands. The 2D networks are extended into 3D supramolecular structure *via* hydrogen bonding between water molecules and the carbonyl oxygen of tartrate anions. The coordinated and uncoordinated water molecules are connected *via* O−H···O hydrogen bond to each other and form six-membered chain water clusters. Moreover, the electrochemical behaviors demonstrate the potential applications in the electrochemical field. Also potentiometric studies confirmed the formation of 2:2 (tart/Cu^{2+}) binary species in the presence of some ternary species in the solution.

References

Al-Dajani, M.T.M., Abdallah, H.H., Mohamed, N., Hemamalini, M., Fun, H.-K., 2010. Acta Crystallogr. E66, m774–m775.

Attar Gharamaleki, J., Aghabozorg, H., Derikvand, Z., Olmstead, M.M., Shokrollahi, A., Aghaei, R., Shamsipour, M., 2011. J. Iran. Chem. Soc. 8, 734–749.

Atwood, J.L., Barbour, L.J., Ness, T.J., Raston, C.L., Raston, P.L., 2001. J. Am. Chem. Soc. 123, 7192–7193.

Brown, H.C. et al, 1955. In: Braude, E.A., Nachod, F.C. (Eds.), Determination of Organic Structures by Physical Methods. Academic Press, New York.

Bruker, 2007. Programs APEX2, SAINT and SADABS. Bruker AXS Inc., Madison, Wisconsin, USA.

Batten, S.R., Robson, R., 1998. Angew. Chem., Int. Ed. 37, 1460–1494.

Du, Y.E., Han, Z.B., 2011. Russ. J. Coord. Chem. 37, 506–510.

Eddaoudi, M., Moler, D.B., Li, H., Chen, B., Reineke, T., OKeeffe, M., Yaghi, O.M., 2001. Acc. Chem. Res. 34, 319–330.

English, J.B., Martell, A.E., Motekaitis, R.J., Murase, I., 1997. Inorg. Chim. Acta 258, 183–192.

Evans, O.R., Ngo, H.L., Lin, W.B., 2001. J. Am. Chem. Soc. 123, 10395–10396.

Férey, G., 2008. Chem. Soc. Rev. 37, 191–214.

Fujita, M., Kwon, Y.J., Washizu, S., Ogura, K., 1994. J. Am. Chem. Soc. 116, 1151–1152.

Holman, K.T., Pivovar, A.M., Ward, M.D., 2001. Science 294, 1907–1911.

James, S.L., 2003. Chem. Soc. Rev. 32, 276–288.

Jian, F., Zhap, P., Wang, Q., 2005. J. Coord. Chem. 58, 1133–1138.

Joannopoulous, J.D., 2001. Nature 414, 257–258.

Kepert, C.J., Prior, T.J., Rosseinsky, M.J., 2000. J. Am. Chem. Soc. 122, 5158–5168.

Kitagawa, S., Kitaura, R., Noro, S., 2004. Angew. Chem., Int. Ed. 43, 2334–2375.

Martell, A.E., Motekaitis, R.J., 1992. Determination and Use of Stability Constants, second ed. VCH, New York.

McCanq, M., Humphreys, F., McKee, V., 1997. Polyhedron 16, 3655–3661.

Meng, X., Shi, J.-C., Tong, Q., Liu, P., Jia, L., 2008. J. Coord. Chem. 61, 3549–3555.

Mirzaei, M., Eshtiagh-Hosseini, H., Alfi, N., Aghabozorg, H., Attar Gharamaleki, J., Beyramabadi, S.A., Khavasi, H.R., Salimi, A.R., Shokrollahi, A., Aghaei, R., Karami, E., 2011a. Struct. Chem. 22, 1365–1377.

Mirzaei, M., Eshtiagh-Hosseini, H., Lippolis, V., Aghabozorg, H., Kordestani, D., Shokrollahi, A., Aghaei, R., Blake, A.J., 2011b. Inorg. Chim. Acta 370, 141–149.

Moghimi, A., Sheshmani, S., Shokrollahi, A., Shamsipur, M., Kickelbik, G., Aghabozorg, H., Anorg, A., 2005. Allg. Chem. 631, 160–169.

Moulton, B., Zaworotko, M.J., 2001. Chem. Rev. 101, 1629–1658.

Piispanen, J., Lajunen, L.H.J., 1995. Acta Chem. Scand. 49 (1995), 235–240.

Sajadi, S.A.A., 2010. Adv. Biosci. Biotechnol. 1, 354–360.

Sawaki, T., Dewa, T., Aoyama, Y., 1998. J. Am. Chem. Soc. 120, 8539–8540.

Seo, J.S., Whang, D., Lee, H., Jun, S.I., Oh, J., Jeon, Y.J., Kim, K., 2000. Nature 404, 982–986.

Sharif, M.A., Aghabozorg, H., Shokrollahi, A., Kickelbick, G., Moghimi, A., Shamsipur, M., 2006. Polish J. Chem. 80, 847–863.

Sheldrick, G.M., 2008. Acta Crystallogr. A64, 112–122.

Shi, W., Chen, X.-Y., Zhao, B., Yu, A., Song, H.-B., Cheng, P., Wang, H.-G., Liao, D.-Z., Yan, S.-P., 2006. Inorg. Chem. 45, 3949–3957.

Synoradzki, L., Bernas, U., Ruskowski, P., 2008. Org. Prep. Proced. Int. 40, 163–200.

Vittal, J.J., 2007. Coord. Chem. Rev. 251, 1781–1795.

Wu, C.D., Lu, C.Z., Lin, X., Wu, D.M., Lu, S.F., Zhuang, H.H., Huang, J.S., 2003. Chem. Commun. 11, 1284–1285.

Zhang, J.P., Chen, X.M., 2008. J. Am. Chem. Soc. 130, 6010–6017.

Zhang, J.P., Huang, X.C., Chen, X.M., 2009. Chem. Soc. Rev. 38, 2385–2396.

Xiong, R.G., You, X.Z., Abrahams, B.F., Xue, Z., Che, C.M., 2001. Angew. Chem., Int. Ed. 40, 4422–4425.